On the QCD phase diagram at finite chemical potential

Lisa M. Haas[*,†], Jens Braun[**] and Jan M. Pawlowski[*,†]

[*]*Institut für Theoretische Physik, Universität Heidelberg, Philosophenweg 16, 69120 Heidelberg, Germany*
[†]*ExtreMe Matter Institute EMMI, GSI, Planckstr. 1, 64291 Darmstadt, Germany*
[**]*Theoretisch-Physikalisches Institut, Universität Jena, Max-Wien-Platz 1, 07743 Jena, Germany*

Abstract. We present results for the phase diagram of QCD with two massless quark flavours as obtained from a first-principles functional renormalisation group approach. In particular we compute order parameters for chiral symmetry breaking and quark confinement at vanishing and non-zero imaginary chemical potential. Our analytical and numerical results suggest a close relation between the chiral and the deconfinement phase transition. We discuss the properties of dual order parameters at imaginary and real chemical potential.

Keywords: QCD phase diagram, imaginary chemical potential, dual order parameter, functional renormalization group
PACS: 05.10.Cc,11.10.Wx,12.38.Aw

One of the unresolved problems in high energy physics is the structure of the QCD phase diagram. This concerns in particular the transition(s) between a deconfined and chirally symmetric phase with microscopic degrees of freedom, quarks and gluons, to a phase of colour-neutral macroscopic bound states, hadrons, with broken chiral symmetry. The deconfinement transition is related to the breaking of the center symmetry of the gauge group and is driven by gluon dynamics. The chiral transition is triggered by strong gluon-induced quark interactions. We report on results of the QCD phase diagram and the relation between the two phase transitions [1]. The question whether both transitions are related is subject of an ongoing debate, see e.g. Refs. [2, 3] for lattice and [4, 5, 6, 7, 8, 9] for model studies.

Approach. We compute the QCD effective action with fRG techniques, which allow us to include all quantum fluctuations step-wise at each momentum scale, for a recent overview see [10]. This is achieved by integrations over small momentum shells, generating a flow from the microscopic action in the UV towards the macroscopic action in the IR. In our two-flavour calculation in the chiral limit [1] we include the Yang-Mills sector of QCD [11, 12] and the matter sector [13, 14, 15, 16] and couple them via dynamic quark-gluon interactions. This approach has already been applied to the chiral phase boundary in one-flavour QCD at finite chemical potential [13]. The confining properties are included via the full momentum dependence of the ghost and gluon propagators [11, 12, 17] and the matter sector incorporates dynamical mesonic degrees of freedom.

Order parameters. The order parameter for the deconfinement phase transition is the Polyakov loop; it is proportional to the energy needed to put a quark into the theory. In our study we implement the Polyakov loop as defined in Ref. [11, 18]. The order parameter for the chiral transition is related to the quark condensate.

Recently so-called dual order parameters for the deconfinement phase transition have been defined [19]. This has been extended in [20] to any observable that transforms non-trivially under center transformations and has been applied in Refs. [21, 22, 23, 24, 25]. An element of the center $Z(N_c)$ of the gauge group is given by $z = \mathbb{1}e^{2\pi i\theta_z}$, where $\theta_z = 0, 1/3, 2/3$ for $SU(3)$. It follows immediately that the sum over all center elements is zero in the symmetric phase and non-zero in the broken phase. This means that any observable that transforms non-trivially under center transformations is an order parameter for confinement.

We have extended the above setting to imaginary chemical potential. It can be incorporated in generalised boundary conditions of the quarks and rewritten in terms of physical quarks with anti-periodic boundary conditions

$$\psi_\theta(x) = e^{2\pi\mathrm{i}\theta_t/\beta}\,\psi(x) \text{ with } \psi(x) = \psi_{\theta=0}(x) \qquad (1)$$

and $\beta = 1/T$. Due to the periodicity in the angle θ, we can Fourier decompose general observables $\mathcal{O}_\theta = \langle \mathcal{O}[e^{2\pi\mathrm{i}\theta_t/\beta}\psi]\rangle$ which depend on the quark fields

$$\mathcal{O}_\theta = \sum_{l\in\mathbb{Z}} e^{2\pi\mathrm{i}l\theta} O_l. \qquad (2)$$

Under center transformations the O_l are multiplied with a center element, $O_l \to z^l O_l$ and hence are order parameters for confinement as they are proportional to the sum over all center elements and thus vanish in the symmetric phase. One example is $\mathcal{L}_\theta = e^{2\pi\mathrm{i}\theta}\langle L\rangle$, where L is the Polyakov loop variable. In particular for $l = 1$ we find

$$\tilde{\mathcal{O}} = \int_0^1 d\theta e^{-2\pi\mathrm{i}\theta}\mathcal{O}_\theta = \int_0^1 d\theta O_1 = O_1. \qquad (3)$$

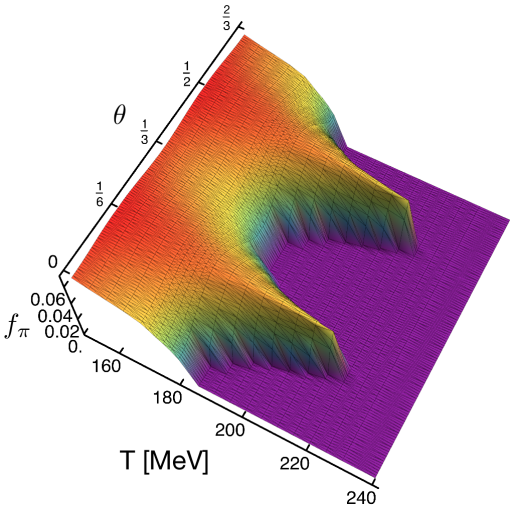

FIGURE 1. The pion decay constant as a function of imaginary chemical potential and temperature.

Thus the dual Polyakov loop in QCD is $\langle L \rangle$.

In general, observables $\mathscr{O}_\theta$ can either be evaluated in QCD with anti-periodic quarks, see e.g. Refs. [19, 20, 21, 22, 23, 24, 25], or in QCD at imaginary chemical potential, QCD_θ, with $\theta-$dependent boundary conditions [1].

The Dirac action with quark fields defined in (1) reads

$$\int \bar{\psi}_\theta \left(i\not{D} + im \right) \psi_\theta , \tag{4}$$

where $\not{D} = \not{\partial} - ig\not{A}$. This can be rewritten such that we obtain an additional term which has the same form as an imaginary chemical potential θ:

$$\int \bar{\psi} \left(i\not{D} + im - 2\pi \frac{1}{\beta} \gamma_0 \theta \right) \psi . \tag{5}$$

Imaginary and real quark chemical potential are related via $\theta = -i\mu\beta/2\pi$. The effective action of QCD is then periodic under a transformation of $\theta \to \theta + \theta_z$: $\mathrm{QCD}_\theta = \mathrm{QCD}_{\theta+\theta_z}$, as the transformation of θ is canceled by the center transformations of the fields. Observables $\mathscr{O}_\theta$ related to the effective action show the same periodicity, namely the Roberge-Weiss (RW) periodicity. However, this also means that if RW periodicity is not broken explicitly, all O_l vanish. The QCD phase diagram at imaginary chemical potential shows a smooth transition until $\theta = 1/6$ but then it displays a discontinuity: the Polyakov loop RW phase transition at T_{RW} [26].

Presence of a fixed background field. The RW periodicity of the generating functional is broken in the presence of a current J. The dual observables O_l then no longer vanish and as derived above, serve as order parameters for confinement. This is implemented by a θ-independent gauge-field background φ. One example of the resulting order parameters is the dual density, which is proportional to the logarithm of the generating functional. Therefore it grows like T^3 at high temperatures as it is proportional to the first moment of the grand canonical potential. Integration by parts yields the fermionic pressure difference $\Delta P(T,\theta) = P(T,\theta) - P(T,0)$.

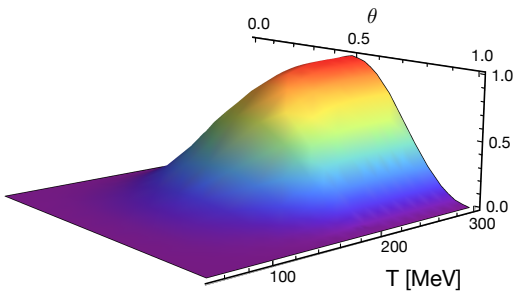

FIGURE 2. $\Delta P(T,\theta)$ as a function of temperature and imaginary chemical potential.

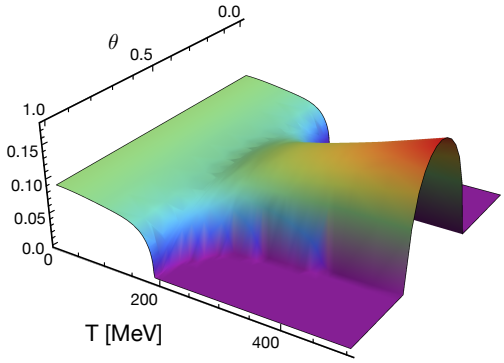

FIGURE 3. The dual quark mass parameter as a function of temperature and imaginary chemical potential.

As the $\mathscr{O}_\theta$ are observables in different theories, distinguished by the boundary condition, the $\tilde{\mathscr{O}}$ vanish only if QCD_θ is in the center symmetric phase for all boundary conditions.

Fig. 2 displays the fermionic pressure difference in the presence of a θ-independent gauge-field background φ. The RW symmetry is broken, however $\theta \to \theta + 1$ still holds. Instead of imaginary chemical potential, one can think of this as an order parameter for different theories which are distinguished by the value of the angle θ.

Another dual observable is the dual quark mass parameter $\tilde{M}[\phi_J]$, see Eq. (3) and $M_\theta[\phi_J]$ in Fig. 3. Due to the presence of a fixed background field it does not vanish in the broken and in the symmetric phase. At $\theta = 1/2$ closely above the phase transition it increases with $\sqrt{T}$ and then linearly as the quarks effectively have bosonic Matsubara frequencies at $\theta = 1/2$. At $\theta = 0$ the dual quark mass is zero above the transition. For vanishing current it is related to the pion decay constant in QCD:

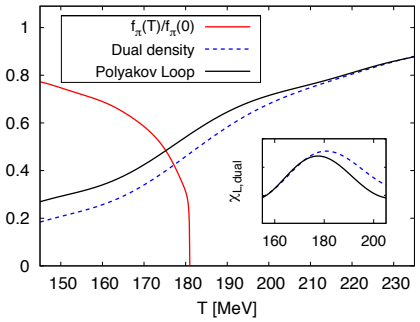

FIGURE 4. The pion decay constant, the dual density and the Polyakov loop as functions of temperature, $\chi_L = \partial_T L$, $\chi_{\mathrm{dual}} = \partial_T \tilde{n}$.

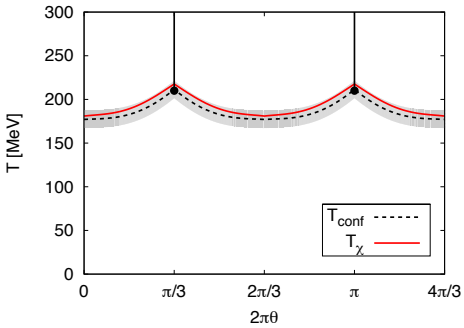

FIGURE 5. The QCD phase diagram at imaginary chemical potential. The grey band represents the width of χ_L. Black dots indicate the endpoints of the Polyakov loop RW transitions.

the slice of the 3D plot at $\theta = 0$ is the (normalised) line shown in Fig. 4.

Results. In our calculation we include the back-reaction of the matter sector on the gauge sector. Moreover, we do not use input from, e. g., lattice calculations to model the gauge dynamics. In other words, the gauge and the matter sector as well as their interplay are treated self-consistently within our approach.

At vanishing chemical potential we consider the order parameters of the chiral and the deconfinement phase transition, the Polyakov loop, the dual density and the pion decay constant, see Fig. 4.

Above $T_c = 180$ MeV the pion decay constant vanishes and chiral symmetry is restored. The dual density and the Polyakov loop both show a peak in their temperature derivative at ≈ 178 MeV. This provides a non-trivial consistency check of our approximation as the Polyakov loop is computed from gluonic correlation functions, whereas the dual density is computed from matter correlation functions. We find that the chiral and the deconfinement transition agree within a few MeV.

Fig. 1 displays the pion decay constant as a function of imaginary chemical potential and temperature. For $T > T_{c,\chi}$ it vanishes and it is non-zero below $T_{c,\chi}$. The RW symmetry is found. Moreover we find a second order phase transition as expected in the chiral limit.

Fig. 5 is a plot of the QCD phase diagram at imaginary chemical potential. The chiral and the deconfinement transition agree within the width of the temperature derivative of the Polyakov loop throughout the phase diagram. The deconfinement transition occurs at lower critical temperatures than the chiral transition. This was also found by lattice computations [27, 28]. First results indicate that this persists at real chemical potential [29].

Acknowledgments. This work is supported by Helmholtz Alliance HA216/EMMI.

REFERENCES

1. J. Braun, L. M. Haas, F. Marhauser, and J. M. Pawlowski, *accepted to Phys. Rev. Lett.* (2010), 0908.0008.
2. Y. Aoki, et al., *JHEP* **06**, 088 (2009).
3. M. Cheng, et al., *Phys.Rev.* **D81**, 054504 (2010).
4. K. Fukushima, *Phys.Lett.* **B591**, 277–284 (2004).
5. C. Ratti, M. A. Thaler, and W. Weise, *Phys.Rev.* **D73**, 014019 (2006).
6. B.-J. Schaefer, J. M. Pawlowski, and J. Wambach, *Phys.Rev.* **D76**, 074023 (2007).
7. Y. Sakai, et al., *Phys.Rev.* **D79**, 096001 (2009).
8. V. Skokov, et al., *Phys.Rev.* **C82**, 015206 (2010).
9. T. K. Herbst, et al. (2010), 1008.0081.
10. J. M. Pawlowski, *these proceedings* (2010).
11. J. Braun, H. Gies, and J. M. Pawlowski, *Phys. Lett.* **B684**, 262–267 (2010).
12. C. S. Fischer, A. Maas, and J. M. Pawlowski, *Annals Phys.* **324**, 2408–2437 (2009).
13. J. Braun, *Eur. Phys. J.* **C64**, 459–482 (2009).
14. H. Gies, and C. Wetterich, *Phys. Rev.* **D69**, 025001 (2004).
15. J. Braun, and H. Gies, *JHEP* **06**, 024 (2006).
16. B.-J. Schaefer, and J. Wambach, *Nucl. Phys.* **A757**, 479–492 (2005).
17. J. Braun, A. Eichhorn, H. Gies, and J. M. Pawlowski, *Eur.Phys.J.* **C70**, 689–702 (2010).
18. F. Marhauser, and J. M. Pawlowski (2008), 0812.1144.
19. C. Gattringer, *Phys. Rev. Lett.* **97**, 032003 (2006).
20. F. Synatschke, A. Wipf, and C. Wozar, *Phys. Rev.* **D75**, 114003 (2007).
21. E. Bilgici, et al., *Phys. Rev.* **D77**, 094007 (2008).
22. E. Bilgici, et al., *Few Body Syst.* **47**, 125–135 (2010).
23. C. S. Fischer, *Phys. Rev. Lett.* **103**, 052003 (2009).
24. C. S. Fischer, A. Maas, and J. A. Muller, *Eur.Phys.J.* **C68**, 165–181 (2010).
25. B. Zhang, et al. (2010), 1012.2314.
26. A. Roberge, and N. Weiss, *Nucl. Phys.* **B275**, 734 (1986).
27. P. de Forcrand, and O. Philipsen, *Nucl. Phys.* **B642**, 290–306 (2002).
28. M. D'Elia, and M.-P. Lombardo, *Phys. Rev.* **D67**, 014505 (2003).
29. J. Braun, L. M. Haas, and J. M. Pawlowski, *work in progress* (2010).